

Fig. 1 Drag coefficient for payload and apogee motor and payload alone.

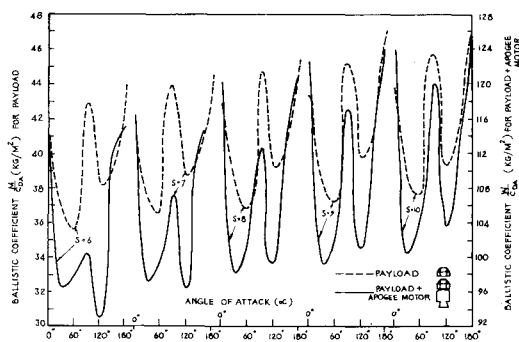


Fig. 2 Ballistic coefficient for payload and apogee motor and payload alone.

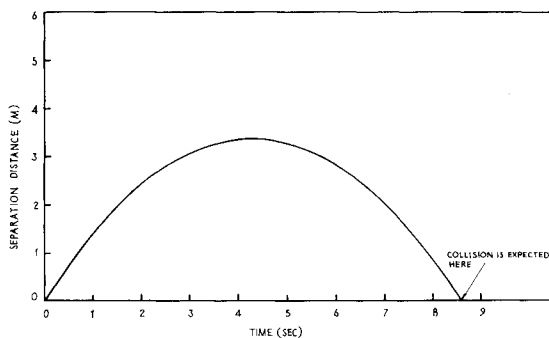


Fig. 3 Time history of separation distance of payload from apogee motor.

satellite has been determined by using Sterne's small perturbation analysis.<sup>2,3</sup>

At altitudes of satellite motion, the intermolecular collisions can be neglected and free molecular flow theory can be used to derive the drag coefficient for geometrically shaped satellites. For a satellite which is made up of plates, the drag coefficient can be computed, taking into account the plate shape combination. The angle of attack ( $\alpha$ ) is the angle between the satellite velocity vector and satellite body axis.

The drag coefficient for a typical polyhedron shaped satellite when the apogee motor has not been separated from the satellite is shown in Fig. 1. It can be seen that the drag coefficient for the combined apogee motor and satellite has been increased by 12% to 38% compared to that of the satellite alone (using the same drag reference area). This is due to the fact that the contribution from the cylindrical apogee motor is much less than that of the polyhedron shaped satellite.

Table 1 Satellite lifetime prediction

	Satellite	Satellite with apogee motor
Weight, kg	35	110
Lifetime, days	246	578
	Apogee	Perigee
Orbit altitudes, km	672.9	289.5

Table 2 Payload and apogee motor mass, c.g., and moment of inertia

	Apogee motor	Payload
Mass, kg	75	35
c.g. location, measured from common c.g., m		
X	-0.2470	0.5060
Y	-0.0025	0.0751
Z	-0.0025	0.0051
Moment of inertia, kg/m <sup>2</sup>		
Ixx	3.6890	1.4522
Iyy	27.3570	1.3222
Izz	27.3570	1.3523
Ixy	0.00	-0.0294
Iyz	0.00	-0.0022
Izx	0.00	-0.0022

The ballistic coefficients for the same configurations, i.e., the configurations for which the drag coefficients have been shown in Fig. 1, are shown in Fig. 2. One can see in Fig. 2 that the ballistic coefficient for the apogee motor and satellite together is 2.28 to 2.81 times higher than that of the satellite alone. This is due to the fact that the weight increases for the satellite and apogee stages together by 3.14 times, while the drag coefficient increases by only 12 to 38%. Since the orbital decay rate is inversely proportional to the ballistic parameter, the orbital decay of the combined satellite and apogee motor will be about 60% less than that of the satellite alone.

The lifetime of a polyhedron shaped satellite alone and in combination with the apogee motor (using the 1966 U.S. standard atmosphere and the drag coefficient shown in Fig. 1) are presented in Table 1. It can be seen from this table that the lifetime increases by 2.36 times if the apogee motor is not separated from the payload.

#### Separation of Payload From Apogee Motor

In the case of satellite separation, the apogee motor may collide with the satellite after separation because tail-off thrust has been acting on the apogee stage for a long time in the near-vacuum conditions existing at the satellite separation altitude. The analysis of a satellite separation has been made by simulating the six-dimensional trajectory of motion of the separating bodies, taking into account the forces and moments due to gravity, thrust, and separation.<sup>5</sup>

The mass and inertia properties of the payload and apogee motor are given in Table 2. The tail-off thrust is assumed to be  $T = 3e^{-0.001t^*}$  where  $t^*$  is the time in seconds measured after apogee motor burnout. The relative distance between the payload and apogee motor after separation is shown in Fig. 3. It can be seen that collision between the payload and apogee motor will occur at about 8.5 s after separation.

For this particular case, the separation must be delayed sufficiently so that the tail-off thrust dies down significantly. The delay of separation will often create unusual operational problems for the ground station. On the other hand, if the apogee motor is not separated from the payload, this problem will not exist, and payload weight gain equal to the separation system weight can be achieved.

## Conclusion

There are distinct advantages of nonseparation of a payload from the apogee motor. However, certain unfavorable implications of this option should also be taken into account. One major problem that has been pointed out is that the apogee motor case may lose its rigidity, and this may lead to coning angle and finally a flat spin. Moreover, this may lead to satellite antenna dip and to thermal imbalance.

## References

- <sup>1</sup>Stafford, W.H. and Craft, R.M., "Artificial Earth Satellite and Successful Solar Probes 1957-1960," NASA TND 601, 1962.
- <sup>2</sup>Biswas, K.K., Thirumalai, K. and Venkataraman, N.S., "Near Earth Satellite Life Time Prediction and Injection Altitude Selection," VSSC-TR-089-78, Vikram Sarabhai Space Centre, Jan. 1978.
- <sup>3</sup>Biswas, K.K., "Effect of Neutral Atmosphere on Spacecraft," *Proceedings of the Environmental Effects on Spacecraft*, Indian Space Research Organization and Indian Institute of Science, Bangalore, India, Education Program, Vol. 2, July 1979.
- <sup>4</sup>Venkataraman, N.S. and Biswas, K.K., "Drag History of RS-2 Satellite," SSTC-ARD-TR-50-73, Vikram Sarabhai Space Center, Trivandrum, India, Nov. 1973.
- <sup>5</sup>Rajeev, Biswas, K.K., and Sasidharan Nair, K.G., "Eulerian Approach for Composite Payload Separation," *Proceedings of the Indian Society of Theoretical and Applied Mechanics*, Vol. 23, Dec. 1978, pp. 38-48.

## A Shuttle Derived Utility Vehicle for Delivery of Small Payloads to Orbit

I.O. MacConochie\* and J.A. Martin\*

NASA Langley Research Center, Hampton, Virginia

E.R. Hischke†

NASA Johnson Space Center, Houston, Texas

and

E.P. Brien‡

Kentron Technical Center, Hampton, Virginia

## Introduction

A DERIVATIVE of the Space Shuttle that results in a vehicle having less capability, but at a reduced cost per flight, is proposed. In this design, the two Solid Rocket Boosters (SRB's) are removed (Fig. 1). The two Shuttle SRB's weigh a total of approximately 2.6 million lb and constitute 57% of the launch weight. After removal of the SRB's, three Space Shuttle Main Engines are added at the rear of the External Tank (ET), and additional main engine propellant tankage is added in the cargo bay. This modified Shuttle is referred to herein as a utility vehicle. It should be noted that the three tank-mounted engines are modified for an expansion ratio of 40 to 1 compared to 77.5 to 1 for the present Shuttle. Only one tank-mounted engine is visible in Fig. 1, since the engines are in line in the side view.

## Mission Description

All six LOX/LH<sub>2</sub> engines are operated at liftoff, giving a thrust-to-weight ratio of 1.3 (Fig. 2). This value varies slightly, depending on the payload and amount of propellant stored in the payload bay. Throttling of the three tank-mounted engines is initiated 93 s after liftoff. Throttling and sequential shutdown of the engines continues until 245 s after liftoff, when all tank-mounted engines are shut down. At this time, throttling of the engines on the Orbiter is initiated while the electrical umbilicals and propellant lines on the tank-mounted engines are separated (a 30 s interval is available for this procedure). At 275 s into the flight, the ET is separated from the Orbiter and is allowed to reenter (Fig. 1). The Orbiter continues on the internal propellants stored in the payload bay. Throttling and sequential shutdown of the engines on the Orbiter proceeds until orbital insertion. After achieving orbit and delivering the payload, the hydrogen tank in the payload bay is discarded to reenter from low-Earth orbit.

The three ET-mounted engines are then retrieved with an extended manipulator arm which is stored in the payload bay. The ET thrust structure is then either collapsed and returned for re-use or expended. The Shuttle returns with the three engines and the cargo bay LOX tank.

In the event of an abort during ascent, the stored propellants in the Orbiter can be burned to depletion with the

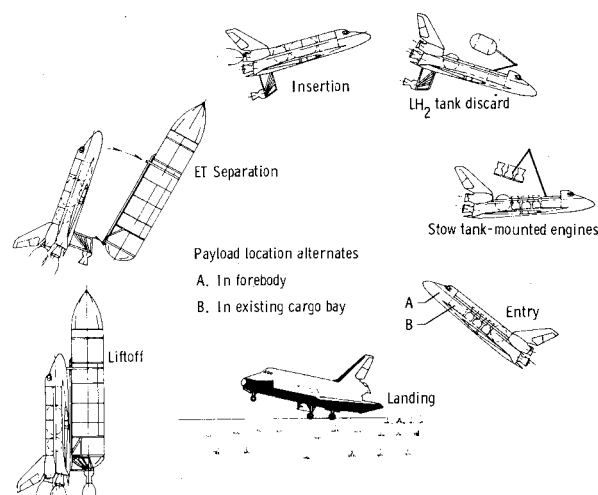


Fig. 2 Thrust, weight, and thrust-to-weight ratio vs time.

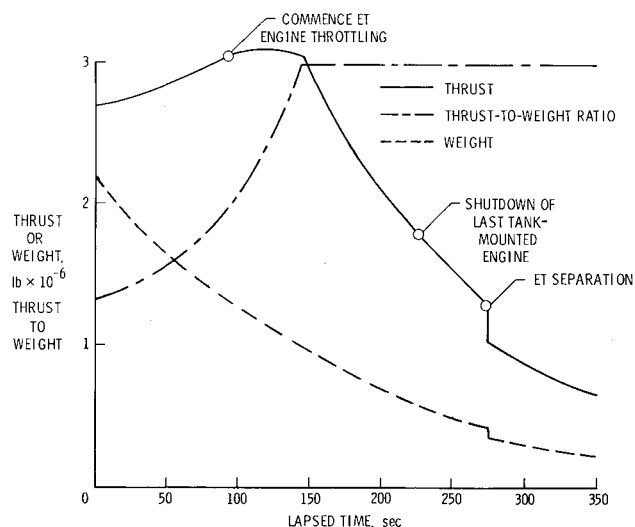


Fig. 1 Utility vehicle configuration and mission sequence.

Received Sept. 8, 1983; revision received Dec. 16, 1983. Copyright © American Institute of Aeronautics and Astronautics, Inc., 1984. All rights reserved.

\*Aerospace Engineer. Member AIAA.

†Aerospace Engineer.

‡Engineering Specialist.